Structural and Electronic Properties of the Charge-Transfer Complex $H_3P\cdots Br_2$ Determined by Fourier Transform Microwave Spectroscopy

E. R. Waclawik and A. C. Legon*[a]

Abstract: The ground-state rotational spectra of six isotopomers of the symmetric-top complex $H_3P\cdots Br_2$ have been measured by the technique of pulsed-nozzle, Fourier transform microwave spectroscopy. The spectroscopic constants B_0, D_J, D_{JK}, $\chi_{aa}(Br_x)$ and $M_{bb}(Br_x)$, x = i (inner) or o (outer) bromine atom, were obtained from analysis of the spectra. Interpretation of these constants with the aid of models revealed that the pre-reactive complex has an intermolecular bond of length $r(P\cdots Br) = 3.0440(4)$ Å between the P atom of PH_3 and one Br atom of Br_2 and that this bond is a relatively strong one, as measured by the intermolecular stretching force constant $k_\sigma = 9.8\ Nm^{-1}$. The complex was discovered to have a significant contribution from charge transfer in the ground state by establishing the fraction of intermolecular charge transferred from P to Br_i [$\delta_i = 0.077(23)$] and the fraction of intramolecular charge transferred from Br_i to Br_o [$\delta_p^{Br} = 0.11(1)$].

Keywords: bromine · charge-transfer · phosphine · rotational spectroscopy

Introduction

Molecular complexes have played an important role in our understanding of modern chemistry since J. D. van der Waals first attempted to explain deviations in behaviour from the ideal gas law by invoking attractive forces between molecules.[1] Molecular complexes that are bound together primarily by dispersion forces are only a small subset of many types of noncovalently bonded molecule in which other forces play a predominant role.[2]

We are currently engaged in a systematic study of the properties of pre-reactive complexes $B\cdots XY$, in which B is a Lewis base and XY is either a homonuclear or heteronuclear dihalogen molecule. These complexes were originally classified as charge-transfer (CT) complexes by R. S. Mulliken.[3] To judge from the parallel behaviour of the angular geometries of series $B\cdots HX$ and $B\cdots XY$, it now seems likely that the angular geometry of $B\cdots XY$ complexes, like those of $B\cdots HX$, are determined in the gas phase largely by the electrostatic part of the interaction between the two subunits of the complex. Methods for the prediction of the likely angular geometries of $B\cdots XY$ complexes have been summarised by a set of empirical rules first proposed for hydrogen-bonded complexes $B\cdots HX$,[4] later extended to "halogen-bonded" complexes.[5, 6]

[a] Prof. Dr. A. C. Legon, Dr. E. R. Waclawik
Department of Chemistry, University of Exeter
Stocker Road, Exeter, EX4 4QD (UK)
Fax: (+44) 1392-263434
E-mail: aclegon@exeter.ac.uk

The focus of the present study is the determination of the structural and electronic properties of the gas-phase pre-reactive complex formed between phosphine and bromine, $H_3P\cdots Br_2$, in the ground electronic state. To this end, the technique of molecular beam Fourier transform microwave (FTMW) spectroscopy was employed to obtain the ground-state rotational spectrum of the complex, but in conjunction with a fast-mixing nozzle to preclude reaction of the two component species prior to measurement. Changes in the rotational constants that occur upon isotopic substitution in B and X_2, obtained from the spectral analysis, were then interpreted to give the positions of the nuclei in the complex.[7]

The strength of the intermolecular bond of the $H_3P\cdots Br_2$ complex was obtained from the spectral constants in the form of the intermolecular stretching force constant k_σ; this value was compared with k_σ in other $B\cdots Br_2$ systems. Comparison of k_σ with other halogen bonded CT complexes $B\cdots XY$, XY = F_2, Cl_2, BrCl, ClF and ICl, has revealed that the magnitude of k_σ depends on the magnitudes of the electric dipole and quadrupole moments of the dihalogen.[6] Thus, the binding strength for a given B complexed to XY is observed to follow the order $F_2 < Cl_2 < Br_2 < ClF \sim BrCl < ICl$.[6]

Significant charge transfer between the components B and XY is most likely to occur when B is a good electron donor (i.e., has a low ionization potential) and XY is a good electron acceptor (i.e., has a strong electron affinity). Significant intermolecular charge transfer in $H_3P\cdots Br_2$ was therefore likely to occur, as both criteria are satisfied. A particular goal of this investigation was to determine accurately the intermolecular transfer of electronic charge (i.e., $\delta_i e$) from H_3P to

  0947-6539/00/0621-3968 $ 17.50+.50/0

Br_2 and to determine the intramolecular redistribution of electronic charge (i.e., $\delta_p^{Br}e$) within Br_2 that occurs when the two components form the complex. Any changes in the distribution of electrons in the component molecules alter the electric field gradients at each nucleus. The atoms that posses a quadrupolar nucleus (Br in $H_3P\cdots Br_2$) will therefore have a different nuclear quadrupole coupling constant from the free Br_2 molecule value. Changes in the Br_2 nuclear quadrupole coupling constants that were extracted from the $H_3P\cdots Br_2$ ground-state rotational spectral data were interpreted by using the Townes–Dailey model[8, 9] for relating electronic structure to observed coupling constants to obtain quantitative measures of δ_i and δ_p^{Br}. The results are compared with δ_i and δ_p^{Br} of other $B\cdots Br_2$ complexes and conclusions drawn about the nature of the $B\cdots Br_2$ interaction.

Results

Spectral analysis: The pattern of the observed rotational lines of $H_3P\cdots Br_2$ corresponded to that of a prolate symmetric top with the P nucleus and two Br nuclei aligned along the unique axis (i.e., the *a* axis). The rotational spectrum exhibited a complicated nuclear quadrupole hyperfine structure arising from the presence of axial Br atoms, both of which have the nuclear spin quantum number $I=3/2$. Only $K=0$ and $K=1$ transitions were detected in the free-jet expansion. This observation implies that rotational energy transfer from the higher energy $K>1$ states is efficient, whereas transfer between $K=1$ and $K=0$ states is spin forbidden.[10] The population of higher J and K rotational states is rapidly transferred to the $K=0$ and $K=1$ levels, from which no further rotational energy transfer takes place.

Rotational constants were extracted from the spectra by using an iterative, nonlinear least-squares fit of an appropriate Hamiltonian to the observed rotational transition frequencies, with exact diagonalisation, by using the program developed by Pickett.[11] The complete matrix of the rotational Hamiltonian is given by Equation (1), in which x represents either the inner (i) or outer (o) bromine atom. The matrix was constructed in the coupled basis $\mathbf{F}_1=\mathbf{J}+\mathbf{I}_{Br_i}$, $\mathbf{F}=\mathbf{F}_1+\mathbf{I}_{Br_o}$ and diagonalised in blocks of *F*. Matrix elements of the Hamiltonian H_R are given by the familiar Equation (2). The nuclear electric quadrupole coupling for each bromine atom was represented by the operator defined in Equation (3), while the operators for the magnetic spin-rotation interaction of each bromine atom were given by Equation (4).

$$H=H_R+\Sigma_x H_Q(Br_x)+\Sigma_x H_{SR}(Br_x) \quad (1)$$

$$H_R=B_0\mathbf{J}^2-D_J\mathbf{J}^4-D_{JK}\mathbf{J}^2J_a^2 \quad (2)$$

$$H_Q=-\tfrac{1}{8}\mathbf{Q}_{Br}:\nabla\mathbf{E}_{Br} \quad (3)$$

$$H_{SR}=\mathbf{I}_{Br}\mathbf{M}_{Br}\mathbf{J} \quad (4)$$

Observed nuclear hyperfine frequencies of the $J+1\leftarrow J$, $K\leftarrow K$ ($J=5$, 6) transitions of the $H_3P\cdots{}^{79}Br^{79}Br$, $H_3P\cdots{}^{81}Br^{79}Br$, $H_3P\cdots{}^{79}Br^{81}Br$ and $H_3P\cdots{}^{81}Br^{81}Br$ isotopomers are presented in Table 1. The observed $J+1\leftarrow J$, $K\leftarrow K$ ($J=6$, 7) transition frequencies of $D_3P\cdots{}^{79}Br^{79}Br$ and $D_3P\cdots{}^{81}Br^{79}Br$ are presented in Table 2. The residuals $\Delta\nu=\nu_{obs}-\nu_{calcd}$ from the final cycles of the fits to experiment are also given in Tables 1 and 2.

The fitted $H_3P\cdots Br_2$ ground-state spectroscopic constants are listed in Table 3 along with the standard deviation σ for each fit. The standard deviations are all smaller than the estimated experimental accuracy of 2 kHz, confirming that only B_0, D_J, D_{JK}, χ_{aa} and M_{bb} terms were necessary to reproduce the rotational spectrum. M_{aa} was not determined from the available data and was preset to zero. Our assumptions that H_R could be truncated after quartic terms in the angular momentum operators and that centrifugal distortion effects upon nuclear quadrupole coupling were not significant were thus valid.

Geometry of $H_3P\cdots Br_2$: As mentioned in the spectral analysis, the observed pattern of rotational lines for the different isotopomers of $H_3P\cdots Br_2$ was characteristic of a prolate symmetric top in which the $P\cdots Br_iBr_o$ nuclei lie along the *a* axis (i represents the inner and o represents the outer bromine atom, respectively). Assuming the complex is formed with a C_{3v} geometry $H_3P\cdots Br_iBr_o$, the moments of inertia of the $H_3P\cdots{}^{79}Br^{79}Br$ complex were modelled initially by taking the component molecule geometries as unchanged from the isolated monomer values. The $P\cdots Br_i$ bond length was then adjusted to reproduce the experimentally observed rotational constant B_0. Substitution of the three hydrogens by deuterons in the model predicted the B_0 of $D_3P\cdots{}^{79}Br^{79}Br$ to within 3 MHz of the observed value, which is a close match considering that large changes in the zero-point motion usually accompany D/H substitutions.

Alternative complex geometries, apart from not making chemical "sense", do not predict values of B_0 for isotopically substituted species in agreement with experiment. For example, substitution of D for H in a model in which the hydrogens of PH_3 lie between the inner Br nucleus and the P nucleus (i.e., $PH_3\cdots{}^{79}Br^{79}Br$) predicts a B_0 value for $PD_3\cdots{}^{79}Br^{79}Br$ that is 23 MHz greater than the experimentally observed quantity given in Table 3.

Isotopic substitution at the bromine nuclei allowed a partial r_s structure of the complex to be established, from which an estimate of any elongation of the *r*(Br–Br) bond length upon complex formation could be made. Unfortunately, since values for the rotational constant A_0 in the various $H_3P\cdots Br_2$ isotopmers cannot be obtained from analysis of only $\Delta K=0$ transitions in a symmetric top, we were unable to establish the positions of the hydrogen atoms in $H_3P\cdots Br_2$ by means of a r_s structure analysis.

The r_s coordinate a_A of an axial atom in a prolate symmetric top is given by Equation (5), in which $\Delta I_b=I_b'-I_b$ is the change in the moment of inertia and $\mu_s=\Delta mM/(\Delta m+M)$ is the reduced mass for the substitution. Taking $H_3P\cdots{}^{79}Br^{79}Br$ as the parent isotopomer and by using the rotational constants for $H_3P\cdots{}^{79}Br^{79}Br$, $H_3P\cdots{}^{81}Br^{79}Br$ and $H_3P\cdots{}^{79}Br^{81}Br$ given in Table 3, the r_s coordinates of Br_i and Br_o were obtained from Equation (5).

$$a_A^2=\Delta I_b/\mu_s \quad (5)$$

  0947-6539/00/0621-3969 $ 17.50+.50/0

Table 1. Observed transition frequencies of the four isotopomers $H_3P\cdots{}^{79}Br^{79}Br$, $H_3P\cdots{}^{81}Br^{79}Br$, $H_3P\cdots{}^{79}Br^{81}Br$ and $H_3P\cdots{}^{81}Br^{81}Br$.

$J' \leftarrow J''$	K	F_1'	$F' \leftarrow F_1''$	F''	$H_3P\cdots{}^{79}Br^{79}Br$		$H_3P\cdots{}^{81}Br^{79}Br$		$H_3P\cdots{}^{79}Br^{81}Br$		$H_3P\cdots{}^{81}Br^{81}Br$	
					ν_{obs} [MHz]	$\Delta\nu$ [kHz][a]	ν_{obs} [MHz]	$\Delta\nu$ [kHz][a]	ν_{obs} [MHz]	$\Delta\nu$ [kHz][a]	ν_{obs} [MHz]	$\Delta\nu$ [kHz][a]
5 ← 4	0	13	16 ← 11	14	7063.0222	0.6	7060.3274	− 2.4	6993.0457	1.4	6990.1009	1.2
	0	13	14 ← 11	12	7070.4749	1.4	7067.3906[b]	0.4	6999.0065	0.9	6996.3697	1.4
	0	13	12 ← 11	10	7073.3107	− 0.5	7067.3906[b]	7.7	7001.1750	− 0.2	6998.8885	− 0.3
	0	13	10 ← 11	8	–	–	7068.7113	− 2.6	6999.5570	1.5	6996.8709	− 3.0
	0	11	14 ← 9	12	7055.0825	− 3.4	7052.8627	− 1.4	6986.6610	− 0.4	6983.4850	− 0.1
	0	11	12 ← 9	10	7067.0909	0.6	7064.1237	0.7	6996.7780	0	6993.6112	3.2
	0	11	10 ← 9	8	7069.1383	1.4	7065.9672	1.6	6998.6973	− 0.7	6995.2957	0.2
	0	11	8 ← 9	6	–	–	–	–	–	–	6998.0875	0.5
	0	9	12 ← 7	10	7071.8889	− 0.1	7070.9250	− 2.4	7002.7869	3.6	6997.6164	0.8
	0	9	10 ← 7	8	7088.3487	− 0.9	7083.5988	1.6	–	–	7011.4711	0.8
	0	9	8 ← 7	6	7074.0974	0.2	7070.6184	0.6	–	–	6999.5350	− 3.7
	0	9	6 ← 7	4	–	–	7065.3179	0.4	6999.4578	− 2.9	6995.0670	− 0.2
	0	7	10 ← 5	8	7072.6782	1.6	7068.1515	1.2	7003.0593	− 1.9	6998.2757	1.2
	1	13	16 ← 11	14	7057.0580	− 0.2	7054.8495	1.7	6987.5112	0.3	6985.0500	− 0.9
	1	13	14 ← 11	12	7070.2252	0.1	7067.1871	− 1.9	6998.6092	1.3	6996.1497	− 1.1
	1	13	12 ← 11	10	7072.1829	− 0.2	7067.6377	− 1.3	6999.7927	− 1.2	6997.8654	− 1.4
	1	13	10 ← 11	8	7061.1526	− 4.6	7059.1992	− 0.1	6990.8958	− 1.6	6988.6167	0.2
	1	11	14 ← 9	12	7060.9667	− 0.1	7058.2527	− 1.4	6992.3015	− 0.3	6988.4928	− 1.1
	1	11	12 ← 9	10	7078.9809	2	7074.9601	2.3	7007.7295[b]	− 3.9	7003.5212	0.1
	1	11	10 ← 9	8	7078.8851	0.7	7074.8488	3.9	7007.7295[b]	7.3	7003.4363	6.6
	1	11	8 ← 9	6	7070.9511	4.4	–	–	–	–	6996.9735	− 2.8
	1	9	12 ← 7	10	7072.2704	0.6	7069.8842	− 0.6	7003.4066	− 5.8	6997.8440	− 5.2
	1	9	10 ← 7	8	7093.5721	− 1.4	7088.3114	1.7	–	–	–	–
	1	9	8 ← 7	6	–	–	–	–	7009.2667	1.3	7005.1469	2.1
	1	9	6 ← 7	4	–	–	7065.7910	− 1.6	7000.0500	− 0.7	6995.4645	− 0.7
	1	7	10 ← 5	8	7061.9660	− 2.2	7058.9069	− 0.5	6992.6607	0.9	6989.3440	− 1.2
	1	7	8 ← 5	6	–	–	7066.0515	− 3.6	7010.0047	0.5	7008.6885	− 2.3
	1	7	4 ← 5	2	–	–	–	–	7001.3514	2.4	6997.7855	5.4
6 ← 5	0	15	18 ← 13	16	8478.9869	2.4	8475.4844	− 0.8	8394.7695	0	8390.9663	0.8
	0	15	16 ← 13	14	8484.4161	1.3	8480.6833	− 0.4	8398.9515	− 1.1	8395.5304	1.3
	0	15	14 ← 13	12	8485.9475	− 0.6	8480.7614	− 0.9	8400.3743	− 0.1	8396.8959	2.5
	0	15	12 ← 13	10	8484.6471	− 0.3	8481.3384	− 0.4	8399.4111	− 0.8	8395.7540	− 1.1
	0	13	16 ← 11	14	8473.2618	0.4	8470.0429	1.6	8390.3324	1.6	8386.1927	0.8
	0	13	14 ← 11	12	8481.0346	− 1.5	8477.4017	0.9	8396.6593	1.8	8392.7419	1.9
	0	13	12 ← 11	10	8483.6956	1.3	8479.8234	0.5	8399.1165	− 1.6	8394.9587	− 3.9
	0	13	10 ← 11	8	8486.2143	− 2.9	8491.0694	− 0.4	8402.9722	− 2.1	8397.0752	− 0.3
	0	13	14 ← 11	14	8622.0086	− 1.4	8607.3101	− 4.1	8520.2395	0.7	8510.3340	0.1
	0	11	14 ← 9	12	8485.5846	2.6	8482.6921	− 2	8401.7866	− 2	8396.5607	0.9
	0	11	12 ← 9	10	8494.4376	1.3	8489.6873	0.3	8409.0237	− 0.1	8404.0197	1.5
	0	11	10 ← 9	8	8488.9802	0.6	8484.7266	5.6	8403.8839	0.6	8399.4547	2.5
	0	11	8 ← 9	6	8483.4712	2.3	8479.4690	− 1.4	8400.0539	− 2.2	–	–
	0	9	12 ← 7	10	8485.7023	–7.6	8481.0041	1.5	8401.6985	1.7	8396.6593	− 2.7
	0	9	10 ← 7	8	8494.5534	0.1	–	–	8407.8314	1.4	8404.0739	− 1.7
	0	9	8 ← 7	6	8507.0776	2.9	8501.4297	0.1	8419.6841	1	8414.5477	− 0.2
	0	9	6 ← 7	4	8495.4034	− 1.9	8490.5602	− 2.4	8409.9919	− 2.5	8404.8405	0.0
	0	9	8 ← 7	8	8420.6665	2.6	–	–	8350.9800	3.8	–	–
	0	9	6 ← 7	6	–	–	8373.9204	− 0.7	–	–	–	–
	0	13	16 ← 13	16	8712.6237	− 3.8	8686.9222	− 0.1	8617.8892	− 1.5	8586.1373	− 0.7
	0	11	12 ← 11	12	8424.1161	1.4	8425.3574	− 1.7	8343.0607	0.5	8344.7051	− 3.5
	0	9	8 ← 11	8	–	–	8418.5780	3.7	–	–	–	–
	1	15	18 ← 13	16	8475.2062	− 0.3	8472.0081	0	8391.2635	1.9	8387.7600	− 1.0
	1	15	16 ← 13	14	8484.1865	0.4	8480.4852	− 0.1	8398.6211	0.6	8395.3194	− 0.6
	1	15	14 ← 13	12	8485.3714	− 0.6	8480.8037	− 2.1	8399.5758	1.3	8396.3609	1.9
	1	15	12 ← 13	10	8478.9732	− 3.9	8475.9266	− 0.2	8394.3799	− 3.5	8390.9916	− 6.0
	1	13	16 ← 11	14	8476.1173	− 0.2	8472.6414	0.7	8393.0957	− 0.1	8388.6052	− 1.0
	1	13	14 ← 11	12	8487.6060	0.8	8483.3878	0	8402.7157[b]	3.2	8398.2185	− 0.3
	1	13	12 ← 11	10	8489.1397	2.7	8484.7707	− 1.2	8404.1520	0.7	8399.4875	− 3.2
	1	13	10 ← 11	8	8485.5051	− 4.1	8488.6146	2	8402.7157[b]	− 2.4	–	–
	1	13	14 ← 11	14	8614.1697	3.8	8600.0510	2.1	–	–	8503.8250	− 0.2
	1	11	14 ← 9	12	8485.7351	1.2	8482.1925	0	8402.1532	− 2.9	8396.6322	2.7
	1	11	12 ← 9	10	8498.2073	1	8493.0910	1	8412.4772	0.8	8407.1114	1.1
	1	11	10 ← 9	8	8492.8739	0.4	8488.2319	2	8407.4602	0.6	8402.6385	− 2.0
	1	11	8 ← 9	6	8483.5924	0.6	8479.5337	0.8	8400.2151	0.5	8394.9891	8.4
	1	9	12 ← 7	10	8479.6580	− 0.6	8475.7063	− 1.2	8395.8687	1.1	8391.5972	− 0.4
	1	9	10 ← 7	8	8491.7544	0.5	8480.1105	− 3.3	8404.9030	0.5	–	–
	1	9	8 ← 7	6	8501.1327	0.8	8496.0446	1.2	8414.1460	0	8409.6217	1.5
	1	9	6 ← 7	4	8486.9561	0.1	8482.8517	1.1	–	–	8397.7703	− 0.2

0947-6539/00/0621-3970 $ 17.50+.50/0 *Chem. Eur. J.* **2000**, *6*, No. 21

Table 1. (cont.)

$J' \leftarrow J''$	K	F_1	$F' \leftarrow F_1''$	F''	$H_3P\cdots{}^{79}Br^{79}Br$		$H_3P\cdots{}^{81}Br^{79}Br$		$H_3P\cdots{}^{79}Br^{81}Br$		$H_3P\cdots{}^{81}Br^{81}Br$	
					ν_{obs} [MHz]	$\Delta\nu$ [kHz][a]	ν_{obs} [MHz]	$\Delta\nu$ [kHz][a]	ν_{obs} [MHz]	$\Delta\nu$ [kHz][a]	ν_{obs} [MHz]	$\Delta\nu$ [kHz][a]
6 ← 5	1	9	8 ← 7	8	8422.8306	0.5	–	–	8351.8482	−1	8344.0371	0.0
	1	9	6 ← 7	6	8372.5124	−2.9	8377.6057	−1.4	–	–	–	–
	1	13	16 ← 13	16	8693.0383	1.3	8669.0651	0.1	8599.2424	1.5	8569.6126	−0.3
	1	11	12 ← 11	12	8434.2989	−0.8	8434.6998	−0.7	8352.5106	−1.6	8353.3054	1.3

[a] $\Delta\nu = \nu_{obs} - \nu_{calc}$. [b] Overlapping lines treated as a blended line with 50% weightings of each line in the fit.

Table 2. Observed transition frequencies of $D_3P\cdots{}^{79}Br^{79}Br$ and $D_3P\cdots{}^{81}Br^{79}Br$.

$J' \leftarrow J''$	K	F_1	$F' \leftarrow F_1''$	F''	$D_3P\cdots{}^{79}Br^{79}Br$		$D_3P\cdots{}^{81}Br^{79}Br$	
					ν_{obs} [MHz]	$\Delta\nu$ [kHz][a]	ν_{obs} [MHz]	$\Delta\nu$ [kHz][a]
6 ← 5	0	15	18 ← 13	16	7913.0675	3.2	7911.0356	−2.6
	0	13	16 ← 11	14	7907.3677	1.0	7905.5977	1.9
	1	15	18 ← 13	16	7909.2770	0.7	7907.5511	2.2
	1	13	16 ← 11	14	7910.1638	0.5	7908.1357	−1.5
7 ← 6	0	17	20 ← 15	18	9233.9939	2.6	9231.4566	−0.9
	0	17	18 ← 15	16	–	–	9235.4310	−1
	0	17	16 ← 15	14	9238.9859[b]	8.4	9235.4944	−3.1
	0	17	14 ← 15	12	9238.1874	−0.6	9235.7694	0.1
	0	15	18 ← 13	16	9229.7087	−1.6	9227.3140	1.0
	0	15	16 ← 13	14	9235.1098[c]	1.3	9232.5079	0.1
	0	15	14 ← 13	12	9237.6699	−1.2	9234.8479	1.1
	0	13	16 ← 11	14	–	–	9236.6553	0.6
	0	11	14 ← 9	12	9238.9563	−2.6	9235.5579	−3.3
	0	11	12 ← 9	10	–	–	9235.5342	6.0
	1	17	20 ← 15	18	9231.3834	0.5	9229.0478	−0.3
	1	17	18 ← 15	16	9237.7992	−2.0	9235.1871	1.1
	1	17	16 ← 15	14	9238.5501	1.7	9235.3973	−3.6
	1	17	14 ← 15	12	9234.5434	−4.4	9232.3074	−1.5
	1	15	18 ← 13	16	9231.1567	−0.4	9228.6100	−0.4
	1	15	16 ← 13	14	–	–	9236.0511	3.9
	1	15	14 ← 13	12	9240.9328	2.9	–	–
	1	13	16 ← 11	14	–	–	9236.2952	1.9
	1	13	14 ← 11	12	9246.7946	1.0	–	–
	1	11	14 ← 9	12	9235.1098[c]	−2.4	9232.1546	−1.6

[a] $\Delta\nu = \nu_{obs} - \nu_{calc}$. [b] Not included in the fit. [c] Overlapping lines treated as a blended line with 50% weightings of each line in the fit.

Values for the coordinates were $a_{Br_i} = -0.4095$ Å and $a_{Br_o} = 1.9082$ Å; the signs were chosen to make physical sense. This gave $r_S(Br{-}Br) = 2.3177$ Å in the complex, which is 0.0344 Å longer than the experimentally determined value for the free $r_0(Br{-}Br)$ bond length supplied in Table 4.

Note that more figures are quoted than would normally be accepted as significant when comparing r_s and r_o distances. If significant intermolecular and intramolecular charge transfer takes place in $H_3P\cdots Br_2$ then it is likely that $r(Br{-}Br)$ will be greater in the complex than in the free molecule.

The method used to establish the r_{cm} distance between the H_3P and Br_2 sub-units in $H_3P\cdots Br_2$, and thereby $r(P\cdots Br_i)$, makes use of the model illustrated in Figure 1. The model takes into account the contribution of the intermolecular bending modes to the zero-point principal moments of inertia of the complex by describing them in terms of two-dimensional isotropic oscillations θ and ϕ of the monomer components about their respective centres of mass[18], as defined in Figure 1. The relation between r_{cm} and the principal moments of inertia of the complex I_b and the principal moments of inertia of the monomer components $I_b^{H_3P}$, $I_c^{H_3P}$ and $I_b^{Br_2}$ is then given by Equation (6), for which r_{cm} is defined in Figure 1 and $\mu = m_{Br_2}m_{H_3P}/(m_{Br_2} + m_{H_3P})$.

$$I_b = \mu\langle r_{cm}^2\rangle + \tfrac{1}{2}I_b^{H_3P}(1 + \langle\cos^2\theta\rangle) + \tfrac{1}{2}I_c^{H_3P}\langle\sin^2\theta\rangle + \tfrac{1}{2}I_b^{Br_2}(1 + \langle\cos^2\theta\rangle) \quad (6)$$

According to arguments set out under the section on "electronic effects", it is shown that the Br_2 oscillation angle β

Table 3. Ground-state spectroscopic constants of six isotopomers of $H_3P\cdots Br_2$.

Spectroscopic constant	$H_3P\cdots{}^{79}Br^{79}Br$	$H_3P\cdots{}^{81}Br^{79}Br$	$H_3P\cdots{}^{79}Br^{81}Br$	$H_3P\cdots{}^{81}Br^{81}Br$	$D_3P\cdots{}^{79}Br^{79}Br$	$D_3P\cdots{}^{81}Br^{79}Br$
B_0 [MHz]	707.04590 (17)	706.71812 (16)	699.99395 (17)	699.64206 (15)	659.88061 (7)	659.6762 (5)
D_J [kHz]	0.187 (3)	0.186 (2)	0.181 (3)	0.183 (2)	0.166[a]	0.166 (5)
D_{JK} [kHz]	13.30 (5)	13.40 (5)	13.07 (5)	13.04 (5)	15.75 (8)	15.87 (6)
$\chi(Br_i)$ [MHz]	823.5201 (98)	687.943 (14)	823.5313 (80)	687.980 (10)	824.13 (16)	688.12 (12)
$\chi(Br_o)$ [MHz]	719.5661 (87)	719.6295 (15)	601.1275 (83)	605.1609 (96)	716.436 (81)	716.73 (13)
$M_{bb}(Br_i)$ [kHz]	1.8 (2)	1.3 (2)	1.9 (2)	1.6 (2)	1.8[b]	1.3[c]
$M_{bb}(Br_o)$ [kHz]	1.6 (2)	2.3 (2)	1.5 (2)	2.0 (2)	1.6[b]	2.3[c]
σ [kHz][d]	2.09	1.84	1.70	2.40	1.93	2.31
N[e]	62	65	61	63	18	22

[a] $D_3P\cdots{}^{79}Br^{79}Br$ constant D_J fixed to the value obtained for $D_3P\cdots{}^{81}Br^{79}Br$. [b] Constants $M_{bb}(Br_i)$ and $M_{bb}(Br_o)$ fixed at the values obtained for $H_3P\cdots{}^{79}Br^{79}Br$ in the fit. [c] Constants $M_{bb}(Br_i)$ and $M_{bb}(Br_o)$ fixed at the values obtained for $H_3P\cdots{}^{81}Br^{79}Br$ in the fit. [d] Standard deviation of fit. [e] Number of lines included in the fit.

Table 4. Spectroscopic and geometric properties of PH_3 and Br_2.

Isotopomer	B_0 [MHz]	C_0 [MHz]	$\chi(^{79}Br)$ [MHz]	$\chi(^{81}Br)$ [MHz]	r_0 [Å]	Angle α [°]
PH_3	133480.1165(17)[a]	117489.4374(77)[a]	–	–	1.4200[c]	122.8624[c]
PD_3	69471.145(23)[b]	58973.960(556)[b]	–	–	1.4176[c]	122.8514[c]
$^{79}Br^{79}Br$	2456.7[d]	2456.7[d]	810.0(5)[e]	–	2.28326[f]	–
$^{79}Br^{81}Br$	2426.4[g]	2426.4[g]	810.0(5)[e]	676.7(4)[h]	–	–
$^{81}Br^{81}Br$	2396.1[g]	2396.1[g]	–	676.7(4)[h]	–	–
^{79}Br	–	–	769.76[i]	–	–	–
^{81}Br	–	–	–	643.03[i]	–	–

[a] Ref. [12]. [b] Ref. [13]. [c] r_0 geometry obtained by fitting B_0 and C_0 to r_0(P–H) and α and by using a least-squares fit to the I_b^0 values. The angle α is defined as the angle between the C_3 axis of Ph_3 and the P–H bond. [d] Ref. [14]. [e] Ref. [15]. [f] Calculated from $r_0 = \{h/(8\pi^2\mu B_0)\}^{1/2}$ and the appropriate B_0 value. [g] Calculated from $B_0 = \{h/(8\pi^2\mu r_0)\}^{1/2}$ by using the r_0 value of $^{79}Br^{79}Br$, for which isotopomer B_0 is an order of magnitude better determined in ref. [16]. [h] Scaled from the $^{79}Br^{79}Br$ values by multiplying the $\chi_0(^{79}Br)$ value of $^{79}Br_2$ by the ratio $^{81}Q/^{79}Q = 0.8354$ of the nuclear quadrupole moments determined in ref. [17]. [i] Ref. [7].

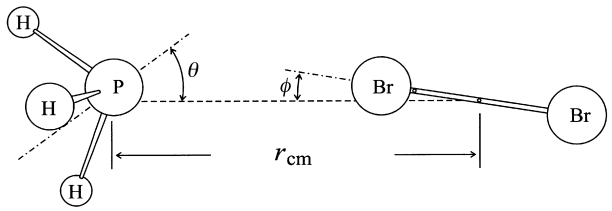

Figure 1. Definition of the distance r_{cm} and the angles θ and ϕ used in the discussion of the geometry of $H_3P\cdots Br_2$.

can be estimated, where β is the angle between the Br_2 internuclear axis and the instantaneous a axis of the complex. Thus we suggest the value $\beta_{av} = \cos^{-1}\langle\cos^2\beta\rangle^{1/2} = 5(2)^\circ$. When averaging is taken properly into account, it can be shown that $\langle\cos^2\phi\rangle = \langle\cos^2\beta\rangle$ and, therefore, ϕ_{av} also lies in the range $5(2)^\circ$.[19] Phosphine has a much smaller reduced mass for the angular oscillation than bromine and can therefore be expected to have a larger oscillation angle θ_{av} in the complex than ϕ_{av} for bromine. An angle of $\theta_{av} = 15^\circ(5)$ was assumed in the model, with the expectation that this range will encompass the actual value of θ_{av}. Fortunately, PH_3 is a near-spherical top and r_{cm} in Equation (6) does not significantly depend upon θ_{av}. The assumed error of 5° caused a change of only 0.0007 Å in r_{cm} and, therefore, in the calculated intermolecular bond distance $r(P\cdots Br_i)$.

Values of I_b, $I_b^{H_3P}$, $I_c^{H_3P}$ and $I_b^{Br_2}$ are obtainable from Tables 3 and 4. The intermolecular bond distance $r(P\cdots Br_i)$ is given by Equation (7), in which r' and r'' are the distances of P and Br_i from the centres of mass of H_3P and Br_2, respectively.

$$r(P\cdots Br_i) = r_{cm} - r' - r'' \quad (7)$$

Values of r_{cm} and $r(P\cdots Br_i)$ for $H_3P\cdots Br_2$, obtained when the assumption of unchanged, isolated monomer bond lengths is made, are given in Table 5. Values are also given in Table 5 for r_{cm} and $r(P\cdots Br_i)$ of $H_3P\cdots Br_2$ calculated by using r_s(Br–Br) and r'' for the elongated Br_2 bond length in the complex, as established by our partial r_s structural analysis. This required use of a predicted $B_s^{Br_2}$ in Equation (6), as re-evaluated by means of the relation $B_s = \{h/(8\pi^2\mu r_s)\}^{1/2}$.

Calculation of the strength of the $H_3P\cdots Br_2$ intermolecular bond: As mentioned briefly in the introduction, the strength of the intermolecular bond in the $H_3P\cdots Br_2$ molecular complex can be measured by the magnitude of the intermolecular stretching force constant k_σ. The quantity k_σ is defined as the restoring force per unit extension of the $P\cdots Br_i$ bond and can be calculated by using the expression for k_σ in a symmetric-top complex given by Millen[20] [Eq. (8)].

$$k_\sigma = (16\pi^2\mu B_0^3/D_J)(1 - B_0/B^{H_3P} - B_0/B^{H_3P}) \quad (8)$$

This equation holds in the approximation of a quadratic force field and of rigid, unchanged component monomer geometries in the molecular complex.[21] Values of D_J, B_0, B^{H_3P} and B^{Br_2} are given in Tables 3 and 4, while μ has been defined in connection with Equation (6). The resulting values for k_σ of the six isotopomers of $H_3P\cdots Br_2$ are identical within experimental error and are listed in Table 5. Use of $B_s^{Br_2}$ for the Br_2

Table 5. Some properties of the complex of $H_3P\cdots Br_2$ determined by rotational spectroscopy.

Isotopomer	r_{cm} [Å][a]	$r(P\cdots Br_i)$ [Å][b]	k_σ [Nm^{-1}][c]	δ_i[d]	δ_p^{Br}[e]
$H_3P\cdots{}^{79}Br^{79}Br$	4.2533 (7)[f]	3.0432 (7)[f]	9.78 (1)	0.080 (23)	0.111 (10)
	4.2271 (7)[g]	2.9997 (7)[g]			
$H_3P\cdots{}^{81}Br^{79}Br$	4.2393 (8)[f]	3.0434 (8)[f]	9.84 (1)	0.077 (23)	0.107 (11)
	4.2126 (7)[g]	2.9997 (7)[g]			
$H_3P\cdots{}^{79}Br^{81}Br$	4.2681 (8)[f]	3.0436 (8)[f]	9.87 (1)	0.077 (23)	0.107 (11)
	4.2416 (7)[g]	2.9997 (7)[g]			
$H_3P\cdots{}^{81}Br^{81}Br$	4.2540 (7)[f]	3.0438 (7)[f]	9.70 (1)	0.077 (22)	0.100 (10)
	4.2272 (8)[g]	2.9998 (8)[g]			
$D_3P\cdots{}^{79}Br^{79}Br$	4.2969 (6)[f]	3.0298 (6)[f]	9.83[h]	0.079 (23)	0.111 (10)
	4.2727 (6)[g]	2.9883 (6)[g]			
$D_3P\cdots{}^{81}Br^{79}Br$	4.2828 (6)[f]	3.0299 (6)[f]	9.78 (3)	0.080 (23)	0.110 (10)
	4.2582 (7)[g]	2.9883 (6)[g]			

[a] r_{cm} determined by using Equation (6). The error in r_{cm} arises from the assumed error in $\theta = \pm 5^\circ$.
[b] $r(P\cdots Br_i)$ determined by using Equation (7). The error in r_{cm} arises from the assumed error in $\theta = \pm 5^\circ$.
[c] Determined from D_J by using Equation (8). The error is that resulting from the experimental error in D_J.
[d] Fraction of an electron transferred from P to Br_i. [e] Fraction of an electron transferred from Br_i to Br_o.
[f] Calculated by using the isolated Br_2 monomer bond length r(Br–Br) and B_0 constants given in Table 4.
[g] Calculated by using the complexed Br_2 bond length r(Br–Br) and B_0 constants determined by r_s analysis of $H_3P\cdots Br_2$ in section on the geometry of $H_3P\cdots Br_2$. See text for discussion.
[h] Calculated by using the assumed value of D_J given in Table 3 for this isotopomer.

0947-6539/00/0621-3972 $ 17.50+.50/0 *Chem. Eur. J.* **2000**, *6*, No. 21

molecule when lengthened in the complex leads to changes of only 0.12 Nm^{-1} in k_o.

Electronic effects—determination of charge transfer in $H_3P\cdots Br_2$: The high precision with which the nuclear quadrupole coupling constants are obtained by FTMW spectroscopy permits the determination of electronic changes that occur in the monomer components upon formation of $H_3P\cdots Br_2$.

As discussed under spectral analysis, the pattern of spectral lines revealed that the complex was a prolate symmetric rotor, where the changes in B_0 of the complex upon deuteration of H_3P showed that the nuclei were aligned in the order $P\cdots Br_iBr_o$ along the symmetric-top axis. The bromine nuclear quadrupole coupling constants can be interpreted by using the Townes–Dailey model of electronic structure to obtain δ_i and δ_p^{Br}, where δ_i is the fraction of an electron transferred from P to Br_i and δ_p^{Br} is the fraction of an electron transferred from Br_i to Br_o.

In the Townes–Dailey model in its simplest form, only valence shell p, d,… electrons centred on a particular nucleus are assumed to contribute to the electric field gradient (efg) at that nucleus. Filled inner shells and valence shell s electrons are taken to retain their spherical symmetry when an atom is incorporated into a molecule. In what follows, we shall consider the changes in the efg's (and hence the nuclear quadrupole coupling constants) of the free Br_2 molecule when the complex $B\cdots Br_i{-}Br_o$ is formed by bringing up a Lewis base B along the Br_2 intermolecular axis z. The subscripts i and o denote the inner and outer Br nuclei, respectively.

In free Br_2, according to the Townes–Dailey model, the efg at each Br nucleus results from a deficit of a single $4p_z$ electron on each atom. If the efg along z in each atom is $-\partial^2V/\partial z^2$ and the atomic nuclear quadrupole coupling constant appropriate to each of a pair of atoms at infinite separation along z is $\chi_A(Br) = (eQ/h)q_A$, in which $q_A = \partial^2V/\partial z^2$ and e is the charge of a proton, it follows that in the free molecule Br_2 the two coupling constants are given by $\chi_0(Br_i) = \chi_A(Br_i) = (eQ_i/h)q_A$ and $\chi_0(Br_o) = \chi_A(Br_o) = (eQ_o/h)q_A$. Note that in earlier publications (e.g., ref. [6] and papers cited therein) definitions of the type $\chi = -(eQ/h)\ \partial^2V/\partial z^2 = -(eQ/h)q_{zz}$ have been used, which correspond to the choice of e as the charge of an electron.

If a $4p_z$ electron were transferred from Br_i to Br_o in covalent Br_2 to give the valence-bond structure $Br_i^+\cdots Br_o^-$, the outer atom achieves the filled shell $4p^6$ and, in the approximation of the Townes–Dailey model, $\chi(Br_o)$ is zero since q_o is zero. On the other hand, the efg at Br_i becomes $q_i = 2q_A$ and hence $\chi(Br_i) = 2\chi_A(Br)$.

We now assume that formation of $B\cdots Br_i{-}Br_o$ leads to a net change $\delta_i - \delta_p^{Br}$ in the fractional population of $4p_z$ electron at Br_i. This change is brought about by the intermolecular transfer of the fraction δ_i of an electron into $4p_z$ on Br_i and the intramolecular transfer of a fraction δ_p^{Br} of an electron from Br_i into $4p_z$ of Br_o. It then follows that the equilibrium nuclear quadrupole coupling constants $\chi_{zz}^e(X)$ at nucleus X, where $X = Br_i$ or Br_o, are related to the free Br_2 values $\chi_0(X)$ by Equation (9), in which $\delta = \delta_i - \delta_p^{Br}$ when $X = Br_i$ and $\delta = \delta_p^{Br}$ when $X = Br_o$. Values of χ_0 and χ_A for the different bromine isotopomers are given in Table 4.

$$\chi_{zz}^e = \chi_0(X) - \delta.\chi_A(X) \quad (9)$$

The zero-point nuclear quadrupole coupling constants $\chi_{aa}(Br_i)$ and $\chi_{aa}(Br_o)$, which are given in Table 3, are to a good approximation related to their equilibrium values $\chi_{zz}^e(Br_i)$ and $\chi_{zz}^e(Br_o)$ by Equation (10), in which P_2 is the associated Legendre polynomial and β is the angle formed between the Br_2 z axis and the a axis of the complex at any instant and the average is over the zero-point motion. Substitution of Equation (10) into Equation (9) leads to Equation (11), in which $\delta = \delta_i - \delta_p^{Br}$ when $X = Br_i$ and $\delta = \delta_p^{Br}$ when $X = Br_o$.

Additionally, when the two bromine nuclei are isotopically identical, it is readily shown that the two equations implied in Equation (11) can be rearranged to Equation (12) and Equation (13) as is the case for $H_3P\cdots{}^{79}Br^{79}Br$, $H_3P\cdots{}^{81}Br^{81}Br$ and $D_3P\cdots{}^{79}Br^{79}Br$.

$$\chi_{aa}(Br) = \chi_{zz}^e(Br)\langle P_2(\cos\beta)\rangle \quad (10)$$

$$\delta = \{\chi_0(X)/\chi_A(X)\} - \{\chi_{aa}(X)/\chi_A(X)\}\langle P_2(\cos\beta)\rangle^{-1} \quad (11)$$

$$\delta_i = 2\{\chi_0(Br)/\chi_A(Br)\} - \{[\chi_{aa}(Br_i) + \chi_{aa}(Br_o)]/\chi_A(Br)\}\langle P_2(\cos\beta)\rangle^{-1} \quad (12)$$

$$\delta_p^{Br} = \{\chi_0(Br)/\chi_A(Br)\} - \{\chi_{aa}(Br_o)/\chi_A(Br)\}\langle P_2(\cos\beta)\rangle^{-1} \quad (13)$$

To obtain values for δ_i and δ_p^{Br} by using Equations (11), (12) and (13) requires knowledge of the angle $\beta_{av} = \cos^{-1}\langle\cos\beta\rangle^{1/2}$. When δ_i was assumed equal to zero in the weakly bound complex $OC\cdots Br_2$[22] analysis of the Br nuclear quadrupole coupling constants gave $\beta_{av} = 6^\circ$. Application of a similar analysis, with the assumption of no charge transfer, to the Br coupling constants of $H_3P\cdots Br_2$ led to a value of $\beta_{av} = 10^\circ$. This is clearly a serious overestimate for β_{av}, since the strength of the intermolecular bond in $H_3P\cdots Br_2$ is a factor of two greater than that of $OC\cdots Br_2$, as evidenced by their k_σ values of $k_\sigma = 9.8\ Nm^{-1}$ and $k_\sigma = 5.0\ Nm^{-1}$, respectively. The more strongly bound complex should undergo smaller amplitude motions, not larger.

A better way to proceed is to assume the β_{av} value for $OC\cdots Br_2$ of 6° is an upper limit for β_{av} in $H_3P\cdots Br_2$ and assume that charge transfer occurs. Considering the relative strengths of the $OC\cdots Br_2$ and $H_3P\cdots Br_2$ intermolecular bonds, a value of $\beta_{av} = 5^\circ(2)$ is likely to encompass the actual value in $H_3P\cdots Br_2$. Fortunately, $\langle P_2(\cos\beta)\rangle$ only varies slowly from unity for a small angles of β[6], so using $\beta_{av} = 5^\circ(2)$ in Equations (11), (12) and (13) should lead to reasonably accurate values of δ_i and δ_p^{Br} in $H_3P\cdots Br_2$. Our estimates of δ_i and δ_p^{Br} obtained by this approach are given in Table 5, where the quoted errors are those generated from our choice of the range in β_{av}.

Discussion

In the preceding sections we have established the structure of $H_3P\cdots Br_2$ to be of C_{3v} symmetry. The nuclei $P\cdots Br_iBr_o$ in the complex were found to be collinear and define the C_3 axis. We have shown that $H_3P\cdots Br_2$ exhibits substantial charge transfer in the ground electronic state. Significant rearrangement of electronic charge was established following interpretation of the bromine nuclear quadrupole coupling constants by using the Townes–Dailey model. Intermolecular transfer of

electronic charge from PH_3 to the inner bromine nucleus of $\delta_i = 0.079\,e$ and intramolecular transfer of electronic charge to from the inner to the outer bromine nucleus of $\delta_p^{Br} = 0.11\,e$ were established. Associated with this rearrangement of electronic structure was an experimentally determined lengthening of the r(Br–Br) bond by about 0.03 Å. Fortunately, although changes in the PH_3 geometry could not be determined by the r_s method, the conclusions present here are insensitive to any such changes.

As defined under the calculation of bond strength, the force constant k_σ is the restoring force per infinitesimal displacement along the dissociation coordinate; it therefore provides a way to order B···XY complexes according to a measure of the strength of binding. The intramolecular electron transfer δ_p^{Cl} from the inner-halogen nucleus to Cl in the extensively studied B···ICl and B···BrCl series exhibited an approximately linear relationship with k_σ.[6] A similar investigation of any systematic variation of the polarisation of Br_2 by the electric field, and its gradients, due to B for the B···Br_2 series of complexes is therefore of interest.

Comparison of δ_p^{Br} versus k_σ in Table 6 reveals that polarisation of the Br_2 subunit within the B···Br_2 complexes increases monotonically with k_σ. The approximately linear dependence of intramolecular charge transfer versus binding strength to the Lewis base appears to be consistent for all complexes B···XY; this holds for both the heteronuclear and homonuclear dihalogen XY. We note that for a given B in Table 6, δ_p^Y does not differ significantly when XY = Br_2 or BrCl. One might expect this trend if δ_p^Y is in-part dependent upon certain properties of the atom X directly involved in the interaction with the Lewis base B, such as the electron affinity or the polarisability of X.

Another notable observation which can be gained by this examination of δ_p versus k_σ in Table 6 is that for the case of B = PH_3 δ_p^Y appears to be anomalously large. This exaggerated polarisation of the XY subunit by PH_3 is apparent for XY = Br_2 and BrCl (Table 6); it has also been observed for the H_3P···ICl complex.[6] This may indicate that the electronic structures of H_3P···XY complexes, XY = Br_2, BrCl and ICl, have a non-negligible contribution from the H_3P^+···XY^- form.

Now that values of δ_i for several B···Br_2 complexes are available we may examine any trends in the intermolecular charge transfer that occur as the Lewis base B is varied. An exponential relationship between δ_i and the first ionisation energy (I_B) of B has previously been identified in the B···ICl series and more recently within the B···BrCl complex series.[6, 23] δ_i is therefore highly correlated with the energy required for removal of an electron from the σ-type nonbonding orbital or a π-bonding orbital of the Lewis base, whichever is directly involved in the interaction. From the limited information available from Table 6, δ_i of the B···Br_2 complexes appear to demonstrate a similar correlation with I_B. The magnitude of δ_i supplied in Table 6 for B···Br_2, increases in the order CO (I_B = 14.0139 eV) < H_2O (I_B = 12.612 eV) < NH_3 (I_B = 9.869 eV) < PH_3 (I_B = 10.16 eV). Clearly the electron donating ability of B, as measured by the ionisation energy, is greatest when the I_B is low. The magnitude of I_B is thus a measure of the distortability, or "softness", of the n-pair electrons of B which significantly influences the amount of intermolecular transfer of electronic charge between the two component molecules of B···Br_2 complexes.

In all the series of halogen-bonded complexes studied by FTMW spectroscopy, B···Cl_2, B···BrCl, B···ClF, B···ICl and now B···Br_2, the intermolecular bond length r(Z···XY) is consistently observed to be shorter than the sum σ(Z) + σ(X) of the van der Waals radii of the electron donor atom and the acceptor atom in the complex. The contraction of the van der Waals radius upon complex formation of Δr = {σ(Z) + σ(X)} − r(Z···X) is given in Table 6 for the four Lewis bases that have been investigated in the B···Br_2 series. In previous studies, the contractions have been in part attributed to anisotropy of the van der Waals radii of the halogen, that is, shorter along the XY internuclear z axis relative to the corresponding radius perpendicular to z.[6, 24] If we compare Δr in the B···Br_2 series with Δr of the hydrogen-bonded B···HBr complexes in Table 6, this anisotropy of the dihalogen van der Waals radius along the internuclear axis is readily apparent. The B···HBr complex internuclear separation r(Z···X) is typically within 0.2 Å of the sum of the appropriate van der Waals radii of the monomers in Table 6, while for the same Lewis bases B, the bromine complexes have large Δr values.

Table 6. Comparison of selected properties of complexes B···Br_2, B···BrCl and B···HBr.

XY	B	r(Z···X)[a]	Δr [Å][b]	k_σ [Nm^{-1}]	δ_i	δ_p^Y
Br_2	CO[c]	3.105	0.55	5.0	0	0.020
	H_2O[d]	2.830	0.52	9.7	0.008	0.051
	PH_3[e]	3.044	0.81	9.8	0.077	0.106
	NH_3[c]	2.72	0.73	18.5	0.06[f]	0.134[f]
BrCl	CO[c]	3.004	0.65	6.3	0.001[g]	0.029[g]
	H_2O[d]	2.882	0.47	12.5	0.009	0.053
	PH_3[g]	2.869	0.98	11.5	0.100	0.128
	NH_3[c]	2.626	0.82	26.7	0.064[g]	0.136[g]
HBr[h]	CO[c]	3.917	0.27	3.0	–	–
	H_2O[i]	3.411	−0.06	10.0	–	–
	PH_3[j]	4.057	0.21	5.0	–	–
	NH_3[c]	3.255	0.20	13.4	–	–

[a] Z represents the electron donor atom in B. X represents the halogen nucleus bonded to Z in the case of XY complexes or Br in the case of HBr. [b] Δr = {σ(Z) + σ(X)} − r(Z···X). Values of the van der Waals radii σ(Z) and σ(X) are from ref. [30]. [c] Value given in ref. [5]. [d] Ref. [31]. [e] This work. [f] Calculated by using the bromine χ_{aa} values and an oscillation angle of 5° in ref. [32]. [g] Calculated by using the BrCl χ_{aa} values and an oscillation angle of 6°, see ref. [23] for justification. [h] Values of δ_i and δ_p^Y could not be determined for B···HBr complexes by the Townes–Dailey model, owing to the large oscillation angles the HBr subunit undergo in these complexes. [i] Ref. [33]. [j] Ref. [34] and ref. [35].

0947-6539/00/0621-3974 $ 17.50+.50/0 *Chem. Eur. J.* **2000**, *6*, No. 21

Comparing Δr for the two dihalogens Br_2 and BrCl with a given Lewis base in Table 6, we find the magnitude of Δr is always larger in the Br_2 complex relative to the BrCl complex by about 0.1 Å. This observation leads us to conclude that the internuclear separation $r(Z\cdots X)$ in the series of complexes is additionally influenced by the magnitude of the electric dipole moment of BrCl. Although the large Δr for $H_3P\cdots Br_2$ observed in this study indicates a distance $r(Z\cdots X)$ that is likely to be energetically unfavourable through the overlapping of the components van der Waals spheres in the complex; this is compensated for by the aforementioned anisotropy and, importantly, the electrostatic forces which hold the complex together.

Experimental Section

The ground-state rotational spectrum of $H_3P\cdots Br_2$ was observed by using a pulsed-jet, cavity microwave (MW) Fourier transform (FT) spectrometer of the Balle–Flygare design.[25] Phosphine (BOC Gases, 99.999%) and bromine (Aldrich) were combined inside the Fabry–Pérot cavity of the spectrometer by using a fast-mixing nozzle.[26] The mixing nozzle avoided the premature reaction of the two gases that would otherwise be expected to occur if a free-jet expansion using components pre-mixed in a conventional stagnation tank at room temperature and pressure had been attempted. A mixture of about 1% PH_3 in Ar was pulsed from a backing pressure of 3 atm through the outer channel of the mixing nozzle by means of a Series 9 solenoid valve (Parker Hannifin) with 0.5 mm inner diameter aperture. Meanwhile, Br_2 was expanded continuously through the near-concentric, coterminous inner glass tube of the mixing nozzle apparatus. The Br_2 flow was adjusted to give a background pressure of 1×10^{-4} mbar inside the spectrometer vacuum chamber during normal operation.

On mixing, the complexes form in three-body collisions at the interface of the expansions; collisional cooling to about 1 K occurs within a few microseconds, when collisionless flow is attained. The direction of flow of our combined free-jet expansions was perpendicular to the direction of MW propagation in the Fabry–Pérot cavity of the apparatus. This perpendicular configuration also minimises Doppler doubling in contrast to a coaxial configuration. This is a distinct advantage when measuring complexes containing bromine, in which many overlapping lines occur in the rotational spectrum due to a rich nuclear quadrupole structure coupled with the overlap of the transitions of several isotopic species. Employing a fast-mixing nozzle in this way has been observed to suppress the splitting of rotational lines by the Doppler effect.

Following expansion, the gas ensemble was polarised and the subsequent free induction decay detected in the usual way.[27] The natural abundance of the two bromine nuclei of 50.5% and 49.5% led to the formation of four possible isotopomers of the $H_3P\cdots Br_2$ complex with nearly equal abundance. The free-jet expansion therefore consisted of about 25% of each isotopomer. Some modifications were made to the apparatus in order increase the signal-to-noise ratio of observed lines by a factor of about 3:1, thus permitting the measurement of weaker $H_3P\cdots Br_2$ nuclear quadrupole components in the rotational spectrum. The isotopic dilution of the number density of a given $H_3P\cdots Br_2$ isotopomer in the free-jet expansion and consequent reduction in signal intensity was compensated for by using a JS-02001800-22-5A Mitec amplifier with noise figure of 2.1 dB and with an IR 02261C1A Mitec image rejection mixer employed to the mix down the molecular emission of frequency ν_m to ν_m+20 MHz, as used by Grabow et al.[28] Rotational transition linewidths of about 16 kHz were typically observed and the accuracy of frequency measurement was estimated to be within about 2 kHz.

Samples of PD_3 were synthesised under vacuum by adding a mixture of DCl (Aldrich, 37% by wt.) in D_2O (Aldrich, >99.92%) dropwise, to Ca_3P_2 (Sigma-Aldrich, 30% by wt.).[29] Evolved PD_3 was condensed at liquid-nitrogen temperature in a glass sample tube. We note that P_2H_4 was also formed by this procedure. Over a 24 hour period an amorphous, yellow polymer formed on the wall of the glass vessel. These factors did not significantly influence the observed intensities of $D_3P\cdots Br_2$ rotational lines.

Acknowledgements

We thank the Leverhume Trust for a research grant in support of this work and EPSRC for the award of a Senior Fellowship to A.C.L.

[1] J. D. van der Waals, Ph.D. Dissertation, Leiden, **1873**.
[2] A. D. Buckingham, P. W. Fowler, J. M. Hutson, *Chem. Rev.* **1988**, *88*, 963–988.
[3] R. S. Mulliken, W. B. Person, *Molecular Complexes*, Wiley-Interscience, New York, **1969**, and references cited therein.
[4] A. C. Legon, D. J. Millen, *Chem. Soc. Rev.* **1987**, *16*, 467–498.
[5] A. C. Legon, *Angew. Chem.* **1999**, *111*, 2850–2880; *Angew. Chem. Int. Ed.* **1999**, *38*, 2686–2714.
[6] A. C. Legon, *Chem. Phys. Lett.* **1999**, *314*, 472–480.
[7] W. Gordy, R. L. Cook in *Microwave Molecular Spectra [Techniques of Organic Chemistry]*, *Vol. 9* (Ed.: A. Weissberger), Interscience, New York, **1970**, Chapter 14.
[8] C. H. Townes, B. P. Dailey, *J. Chem. Phys.* **1949**, *17*, 782–796.
[9] C. H. Townes, A. L. Schawlow, *Microwave Spectroscopy*, McGraw-Hill, New York, **1955**, Chapter 9.
[10] A. C. Legon, *Faraday Discuss. Chem. Soc.* **1988**, *86*, 269.
[11] H. M. Pickett, *J. Mol. Spectrosc.* **1991**, *148*, 371–377.
[12] A. V. Burenin, *Mol. Phys.* **1992**, *75*, 305–309.
[13] A. V. Burenin, S. M. Shchapin, *Opt. Spectrosk.* **1982**, *52*, 375–376.
[14] D. M. Bishop, S. M. Cybulski, *J. Chem. Phys.* **1994**, *101*, 2180–2185.
[15] N. Bettin, H. Knöckel, E. Tiemann, *Chem. Phys. Lett.* **1981**, *80*, 386–388.
[16] R. F. Barrow, T. C. Clark, J. A. Coxon, K. K. Lee, *J. Molec. Spectrosc.* **1974**, *51*, 428– 438.
[17] A. C. Legon, J. C. Thorn, *Chem. Phys. Lett.* **1993**, *215*, 554–560.
[18] G. T. Fraser, K. R. Leopold, W. Klemperer, *J. Chem. Phys.* **1984**, *80*, 1423–1426.
[19] K. R. Leopold, G. T. Fraser, W. Klemperer, *J. Chem. Phys.* **1984**, *80*, 1039–1046.
[20] D. J. Millen, *Can. J. Chem.* **1985**, *63*, 1477–1479.
[21] M. R. Keenan, D. B. Wozniak, W. H. Flygare, *J. Chem. Phys.* **1981**, *75*, 631–640.
[22] E. R. Waclawik, J. M. A. Thumwood, D. G. Lister, P. W. Fowler, A. C. Legon, *Mol. Phys.* **1999**, *97*, 159–166.
[23] A. C. Legon, J. M. A. Thumwood, E. R. Waclawik, *J. Chem. Phys.*, in press.
[24] S. A. Peebles, P. W. Fowler, A. C. Legon, *Chem. Phys. Lett.* **1995**, *240*, 130–134.
[25] T. J. Balle, W. H. Flygare, *Rev. Sci. Instrum.* **1981**, *52*, 33–45.
[26] A. C. Legon, C. A. Rego, *J. Chem. Soc. Faraday Trans.* **1990**, *86*, 1915–1921.
[27] A. C. Legon in *Atomic and Molecular Beam Methods*, *Vol. 2* (Ed.: G. Scoles), Oxford University Press, Oxford, **1992**, Chapter 9.
[28] J.-U. Grabow, W. Stahl, H. Dreizler, *Rev. Sci. Instrum.* **1996**, *67*, 4072–4084.
[29] *Handbook of Preparative Inorganic Chemistry*, *Vol. 1* (Ed.: G. Brauer), Academic Press, New York, **1962**, Section 9, p. 527.
[30] L. Pauling, *The Nature of the Chemical Bond*, Cornell University Press, Ithaca, New York, **1960**, p. 260.
[31] E. R. Waclawik, J. M. A. Thumwood, J. B. Davey, A. C. Legon, unpublished results.
[32] H. I. Bloemink, A. C. Legon, *J. Chem. Phys.* **1995**, *103*, 876–882.
[33] A. C. Legon, A. P. Suckley, *Chem. Phys. Lett.* **1988**, *150*, 153–158.
[34] L. C. Willoughby, A. C. Legon, *J. Phys. Chem.* **1983**, *87*, 2085–2090.
[35] A. C. Legon, D. J. Millen, *J. Am. Chem. Soc.* **1987**, *109*, 356–358.

Received: March 30, 2000 [F2395]

  0947-6539/00/0621-3975 $ 17.50+.50/0